A Novel Stimulus to Improve Perimetric Sampling within the Macula in Patients with Glaucoma

Muhammed S. Alluwimi, PhD, FAAO,[1]* William H. Swanson, PhD, FAAO,[2] and Brett J. King, OD, FAAO[2]

SIGNIFICANCE: Identifying glaucomatous damage to the macula has become important for diagnosing and managing patients with glaucoma. In this study, we presented an approach that provides better perimetric sampling for the macular region, by testing four locations, with a good structure-function agreement.

PURPOSE: We previously presented a basis for customizing perimetric locations within the macula. In this study, we aimed to improve perimetric sampling within the macula by presenting a stimulus at four locations, with maintaining a good structure-function agreement.

METHODS: We tested one eye each of 30 patients (aged 50 to 88 years). Patients were selected based on observed structural damage to the macula, whereas perimetric defect (using 24-2) did not reflect the locations and extent of this damage. We used en face images to visualize retinal nerve fiber bundle defects. To measure perimetric sensitivities, we used a blob stimulus (standard deviation of 0.25°) at the 10-2 locations. A perimetric defect for a location was defined as any value equal to or deeper than –4, –5, and –6 dB below the mean sensitivity for 37 age-similar controls (aged 47 to 78 years). We also presented an elongated sinusoidal stimulus for 20 patients at four locations within the macula, in which we defined a perimetric defect as any value below the 2.5th percentile from controls.

RESULTS: The –4, –5, and –6 dB criteria identified perimetric defects in 14, 13, and 11 patients, respectively. When testing with the elongated stimulus, 18 patients were identified with perimetric defect. The perimetric defects were consistent with the structural damage.

CONCLUSIONS: The elongated stimulus showed a good structure-function agreement with only four testing locations as compared with 68 locations used with the blob stimulus. This demonstrates a clinical potential for this new stimulus in the next generation of perimetry.

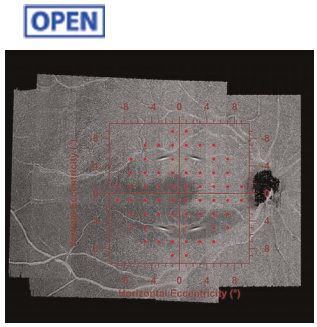

Author Affiliations:
[1]Department of Optometry, College of Applied Medical Sciences, Qassim University, Buraidah, AlQassim, Saudi Arabia
[2]Indiana University School of Optometry, Bloomington, Indiana
*malluwim@indiana.edu

Optom Vis Sci 2021;98:374–383. doi:10.1097/OPX.0000000000001677

It is widely accepted that macular damage occurs at early stages of glaucoma. However, the most commonly used perimetric testing applies the 24-2 grid, which has only four locations (separated by 6° horizontally and vertically) that cover the central ±8° of the retina, defined as macula in this study. This leads to poor sampling of the macula because these four locations are not optimum for detecting damage in this area. During the past decade, several reports concluded that there was a spatial correspondence between structural and perimetric defects within the macula in patients with glaucoma when using 10-2 grid (perimetric locations are separated by 2° horizontally and vertically).[1–5] However, it is challenging for clinicians to use both 24-2 and 10-2 grids at the same visit to examine patients with glaucoma.

Recent efforts investigated alternative approaches such as adding macular test locations to the 24-2 locations and computing pattern standard deviation for only the central 12 perimetric locations of the 24-2 grid, as an index for perimetric defect within the macula.[6] These two approaches, however, did not assess the spatial correspondence of structural and functional measures. A recent report by Hood et al.[7] found that the new index for the macula did not provide good measurement for early defect within the macula and emphasized the importance of spatial comparison between the structural and functional measures in patients with glaucoma.

Perimetric and imaging measurements provide two different types of information, with relatively independent sources of variability in healthy eyes.[8] Phu and Kalloniatis[9] suggested that adding fixed locations to the 24-2 or 10-2 grids may be limited by the anatomical variability among individuals. In a prior study,[10] we found a good structure-function agreement within the macula using en face optical coherence tomography images, as did a recent study from another laboratory.[11] We also proposed the use of customized perimetric locations within the macula. We used a blob stimulus with smooth edges, similar to the size III Goldmann stimulus. Stimuli were presented at the 10-2 locations, which required a large number of perimetric stimuli because of the small stimulus area. However, large sinusoidal stimuli with flickering temporal presentation have been shown to yield similar defects to those observed with the small Goldmann size III stimulus.[12,13] The use of sinusoidal stimuli has potential for sampling macular damage with fewer stimulus presentations.

In the current study, we aimed to refine these findings by using a custom sinusoidal stimulus that allowed for the sampling of much larger retinal regions than the conventional size III stimulus.[14,15] This allowed us to evaluate its clinical potential in the next generation of perimetry by reducing the number of testing locations while maintaining the ability to detect perimetric glaucomatous defects within the macula.

METHODS

Participants

We recruited 30 patients with glaucoma and 37 age-similar control participants from an ongoing glaucoma study. For each participant, the purpose and procedures for the study were explained; an informed consent form was signed by each participant before testing sessions were started. This study was approved by the Indiana University Institutional Review Board. The protocol and procedures for this study adhered to the tenets of the Declaration of Helsinki. The age range for patients with glaucoma was from 50 to 88 years, with a mean (standard deviation) of 69 (7.8) years. The age range for control participants was from 47 to 78 years, with a mean (standard deviation) of 61 (10.6) years.

The patients were selected based on the criterion that there was glaucomatous damage present within the macula as observed on structural measurements, but the perimetric defect did not reflect the locations and extent of structural damage. Any participant who did not meet this criterion was not recruited for the current study. This means that advanced cases of glaucoma were not recruited because glaucomatous damage is deep and wide enough that structural and functional agreement will be in agreement that there is severe damage.

The determination of structural loss was made based on qualitative analysis of the en face images for the retinal nerve fiber bundles, which identified regions of low reflectance as a result of glaucomatous insult (Fig. 1).[10] This qualitative analysis was confirmed by asymmetry analysis of ganglion cell layer thickness using spectral-domain optical coherence tomography. One of the authors was trained on how to evaluate glaucomatous damage to the nerve fiber bundles in which images of more than 50 people free of eye disease (aged 20 to 85 years) and 30 patients with glaucoma were reviewed. Perimetric loss was defined based on the 24-2 data in which at least one location had $P < .5\%$ or at least two adjoining locations had $P < 1\%$ in the total deviation and/or pattern deviation maps. Mean deviation for the patients ranged from –12.7 to +1.4 dB, with a median of –2.8 dB and an interquartile range of –5.5 to –1.5 dB (Fig. 2). We did not include points at the edges of the visual field test locations, as they are more susceptible to unreliable data. Pattern standard deviation for the patients ranged from 1.8 to 15.9 dB, with a median of 4.1 dB and an interquartile range of 2.6 to 8.4 dB.

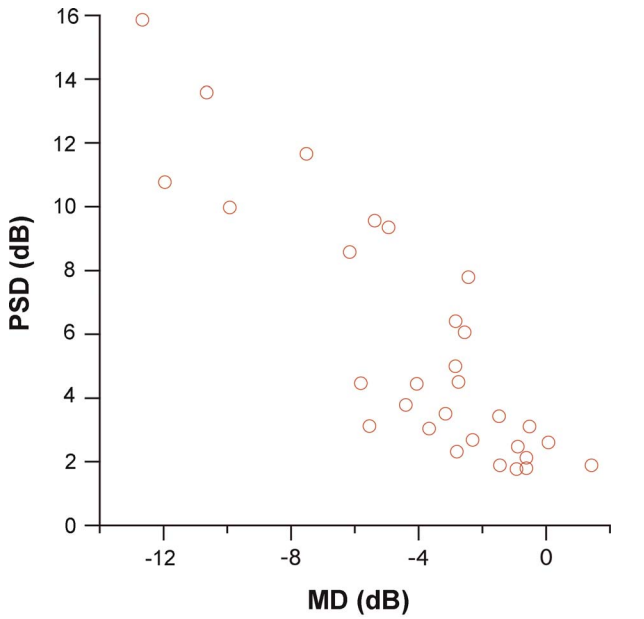

FIGURE 2. The distribution of mean deviation (*x*-axis) and pattern standard deviation (*y*-axis) for the participants recruited in the current study.

Inclusion Criteria

All participants had a comprehensive eye examination with a best-corrected visual acuity of 20/20, except for participants who were 70 years or older in which 20/40 was acceptable. We included participants who had spherical equivalent refractive error

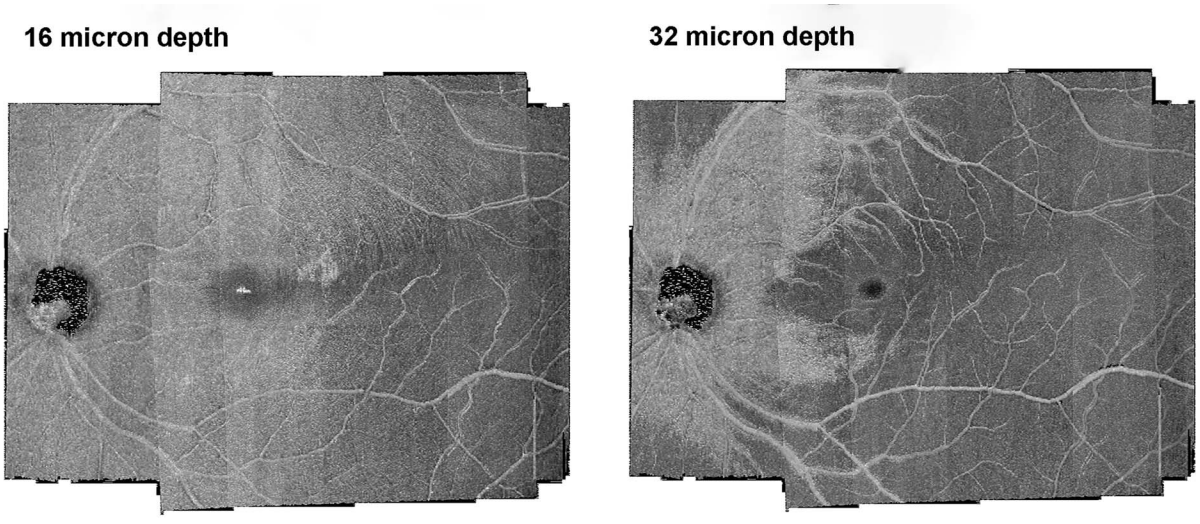

FIGURE 1. Two en face images of retinal nerve fiber bundles, for the same patient, at two different depths from the inner limiting membrane. To avoid shadow artifacts that may be observed on en face view, we computed coefficient attenuation as previously described.[16–18] One can appreciate the retinal nerve fiber layer defect at the inferior region of the temporal raphe at a superficial depth from the inner limiting membrane (16 μm, left) but not at a deeper depth (32 μm, right). In contrast, it can be observed that an inferior wedge defect was not well characterized at the superficial depth (16 μm, left), whereas it was well characterized at the deeper depth (32 μm, right).

between +2.0 and –6.0 D and cylindrical correction ≤±3.0 D. We limited the cylindrical corrections to be between –3.00 and +3.00 D, to reduce the effect of blur.[19] Common inclusion criteria were absence of systemic disease affecting visual function, no history of ocular disease except glaucoma for patients, absence of ocular surgery except uncomplicated cataract surgery or glaucoma surgery for patients, and clear ocular media. Additional inclusion criteria for control participants were open anterior chamber angle and normal cup-to-disc ratio, as defined in the clinical chart, with no evidence of focal narrowing or notching of the neuroretinal rim.

Exclusion Criteria

Common exclusion criteria were the presence of ocular disease affecting visual function (other than glaucoma for the patients) such as diabetic retinopathy, macular degeneration, prior vein occlusion, degenerative myopia, amblyopia, peripheral anterior synechiae, medications affecting visual functions, and epiretinal membrane advanced enough to prevent visualizing nerve fiber bundles. We also excluded participants who had an abnormal appearance of the optic disc or abnormal visual field due to neurological disorders such as stroke or post-chiasmatic disorders, or those who were difficult to image because of poor fixation. An additional exclusion criterion for patients with glaucoma was IOP >30 mmHg under treatment. For control participants, we excluded those who had an IOP greater than 21 mmHg for the last clinic visit, a glaucomatous appearance to the optic nerve head, or abnormal appearance of the fundus.

Study Protocol

For the small blob stimulus, the first 10 patients and the first 10 of the 37 age-similar control participants were tested once because these participants had previously been tested several times in different studies conducted by our laboratory with the customized perimetric testing station. Data for these 10 patients and 10 age-similar control participants were previously published by applying only a single criterion for abnormality (–0.5 log units), whereas for the current study, we also applied alternative criteria for all 37 control participants and all 30 patients with glaucoma to explore the effectiveness of each criterion. Because they were new to the customized perimetric testing station, the remaining 27 control participants and 20 patients with glaucoma were examined in two visits; the first visit served as a testing practice, and the sensitivities from the second visit were used in the analysis. These 20 patients were also tested with the elongated sinusoidal stimulus in the two separate visits.

Equipment

Spectral-domain Optical Coherence Tomography

As previously described,[10] volume files with vertical dense B-scans (30 μm apart) were gathered in high-speed mode using a Spectralis optical coherence tomography (Spectralis OCT version 6.4; Heidelberg Engineering, Heidelberg, Germany). Six overlapping volume scans covered much of the central ±30° of the retina.[20] All participants were dilated to allow for rapid optical coherence tomography scans. The width and height of the first rectangle were 15° × 30° that covered the optic disc and adjacent region; the nasal fixation target was used. The second and third rectangles were each designed to image 10° × 20° regions superior and inferior to the macula using fixation targets above and below the fovea. The fourth and fifth rectangles were 20° × 20°; the temporal superior and inferior fixation targets were used so that the operator imaged temporal superior and inferior regions. The sixth rectangle was 10° × 30°; temporal central fixation was used, and the operator moved the rectangle to the farthest temporal side to image the temporal aspect of the posterior pole.

Volume scans were extracted from the Spectralis and read by a custom MATLAB software program (MathWorks Inc., Natick, MA). This custom program was applied to montage volume scans of the six rectangles into a single volume scan and provided en face images at different depths from the inner limiting membrane. Retinal locations were kept in degrees of visual angle to facilitate comparison with perimetric data.

En face view was used to visualize nerve fiber bundles to identify glaucomatous damage within the macula. However, it was challenging to visualize nerve fiber bundle defects at only one fixed depth from the inner limiting membrane (Fig. 1). This is due to the anatomical organization of nerve fiber bundle density, which led to differences in the nerve fiber layer thickness between the temporal (thinner nerve fiber layer) and nasal regions (thicker nerve fiber layer) of the macula. Therefore, multiple depths from the inner limiting membrane were warranted to identify glaucomatous damage.

Perimetry

We used a customized perimetric station; details were previously described.[14] In brief, we used a cathode-ray tube system, controlled by a visual stimulus generator (ViSaGe; Cambridge Research System, Ltd., Cambridge, United Kingdom), with a screen resolution of 800 × 600 pixels subtending 51° × 42° of visual angle. This system was controlled by a custom MATLAB program. The perimetric station was equipped with a motorized headrest to control head position. A camera was attached to monitor fixation. In addition, a lens holder was attached to the station at a distance of 33 cm in front of the screen; the participant's spherical equivalent correction for this test distance was used for the perimetric testing.

The background luminance was 20 cd/m^2, and the maximum stimulus luminance was 100 cd/m^2, giving a maximum Weber contrast of 400%. We used this background luminance for two reasons. First, the typical 10 cd/m^2 for the background luminance does not provide complete resistance to the effects of reduced retinal illumination because of small pupils or dense lenses[21]; therefore, the higher background luminance should help reduce between-subject variability. Second, the background luminance that we used limits the maximum contrast to 400%, which is equivalent to 19 dB on the Humphrey Field Analyzer (Carl Zeiss Meditec, Dublin, CA). This contrast range reduces the effects of retinal ganglion saturation on test-retest variability.[22–24] The custom testing station that we used provides custom 50-mm spherical lenses in steps of 1 D, so we used stimuli designed to yield contrast sensitivities that are resistant to the effects of modest blur[19] and required that any astigmatism be modest.

Perimetric Stimuli

Blob Stimulus

A blob stimulus was used to measure perimetric sensitivities at the 68 standard 10-2 locations. The blob stimulus was a 2D Gaussian with a standard deviation of 0.25° (Fig. 3) and temporal presentation with a 200-millisecond rectangular luminance increment. A blob stimulus was selected because it does not have the sharp edge of standard circular perimetric stimulus and has been found to reduce test-retest variability and resist the effects of blur.[19,23]

Elongated Sinusoidal Stimulus

The sinusoidal stimulus was an elongated first derivative of Gaussian stimulus (Fig. 3), with peak spatial frequency of 1.0 cycle

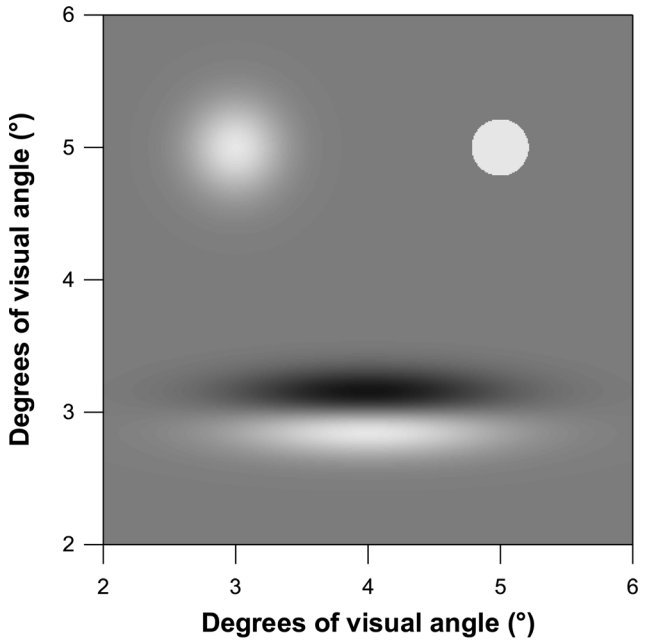

FIGURE 3. Stimuli. (Top left) Blob stimulus, a 2D Gaussian of 0.25° standard deviation. (Top right) Goldmann stimulus size III, to demonstrate the equivalent size of blob stimulus. (Bottom) Elongated sinusoidal stimulus, a first derivative of Gaussian with a peak spatial frequency of 1 cycle per degree. Vertical and horizontal axes show the dimensions in degrees of visual angle.

per degree and an orthogonal Gaussian window with a standard deviation of 0.71°. This produced two adjoining bars, one dark and one light. The temporal presentation was three cycles of 5-Hz counterphase flicker, which means that every 100 milliseconds the bar that was dark became light and the bar that was light became dark, over a total of 600 milliseconds. The dimensions of this stimulus were approximately 3° horizontally and 1° vertically, covering approximately the area of three 10-2 locations. When sinusoidal stimuli with low-spatial-frequency content have been presented to patients with glaucoma at locations of glaucomatous damage, reduced sensitivities have been found at these locations.[25–27] The low spatial frequency was chosen to reduce the effects of peripheral defocus or astigmatism.[19] The flicker rate was chosen to be low enough that contrast sensitivity is expected to adhere to Weber's law[21] and to provide advantages of a large area of cortical pooling.[15] Details of the elongated sinusoidal stimulus used in this study have been previously described.[25]

We used the elongated sinusoidal stimulus to test 20 patients at four perimetric eccentricities (Fig. 4): location 1 (–2.5, +5), location 2 (+2.5, +5), location 3 (–2.5, –5), and location 4 (+2.5, –5) in two separate visits. The determination of these locations was made based on a suggestion by Hood et al.,[28] aiming to enhance the perimetric sampling within the macula. The originally suggested locations were (–1, +5) and (+1, +5), and we mirrored the other locations at the inferior field. Our goal for implementing this stimulus at these locations was to demonstrate the feasibility of improving perimetric sampling within the macula in patients with glaucoma.

The elongated sinusoidal stimulus was placed in locations where the two perimetric presentations would not overlap. If we put this stimulus at the same locations that Hood et al.[28] suggested, there would be an overlap of the retinal regions covered by the two stimuli. Therefore, we shifted the locations by 1.5° horizontally to avoid overlap and still cover the locations suggested by Hood et al.[28] At each location, the elongated sinusoidal stimulus was presented with a similar orientation to that of the nerve fiber bundles in the retinal region being tested. This stimulus has been reported to yield reduced perimetric sensitivities in patients with glaucoma as compared with control participants tested at similar locations and similar orientations.[25]

Statistical Analysis

For the blob stimulus, an abnormality was defined based on the total deviation and pattern deviation maps that were computed relative to the unsmoothed raw data of control participants. The total deviation for each location was computed as the difference from mean sensitivity of the control group at that location. The pattern deviation for each location was computed from total deviation with adjustment for the height of the hill of vision, which was calculated as the seventh highest value of total deviation values for a participant subtracted from the average of the seventh highest total deviation values for the controls. For both total deviation and pattern deviation, values deeper than –0.5 log units were considered defects, as in our prior study,[10] and the effects of this choice were evaluated by using alternates of –0.4 and –0.6 log units. An abnormality for the blob stimulus was defined as at least two adjoining perimetric locations with defect deeper than each criterion defined previously.

For the elongated sinusoidal stimulus, perimetric defect for each location was defined as any perimetric sensitivity that fell below the 2.5th percentile for control participants, as in our prior study. The abnormality for the elongated sinusoidal stimulus was defined as at least one perimetric location that had a perimetric defect as defined previously. To compare the performance of each stimulus (elongated as compared with blob) in identifying perimetric defects in the 20 patients, we computed the 2.5th percentiles for the blob stimulus data (Fig. 7). Then, a gray scale was created for total deviation and pattern deviation maps, and the results were compared with those found using –0.4, –0.5, and –0.6 cutoffs in terms of how many patients with glaucoma were identified.

To better visualize the pattern of perimetric defect, we restricted the range for the total deviation and pattern deviation values for the gray scale to start from –0.25 log units as the minimum value to –0.7 log units as the maximum value. The minimum value was defined based on the 2.5th percentile of the control participants for blob stimulus data. To identify a perimetric defect with the gray scale, we required that at least two contiguous perimetric locations in total deviation or pattern deviation maps had values that fell below the defined minimum.

To evaluate the correspondence between structure and function in patients with glaucoma, results of perimetric tests using the blob stimulus were superimposed on en face images of the nerve fiber bundles. The superimposition was obtained by centering fixation (0° location) on the fovea based on the foveal reflectance observed on the en face view and rotating the montage (if needed) to align the optic nerve with the location of the blind spot as found in prior perimetric examinations using a standard 24-2 grid.

RESULTS

Table 1 shows results for the different criteria used with the blob stimulus. The perimetric defects were consistent with the

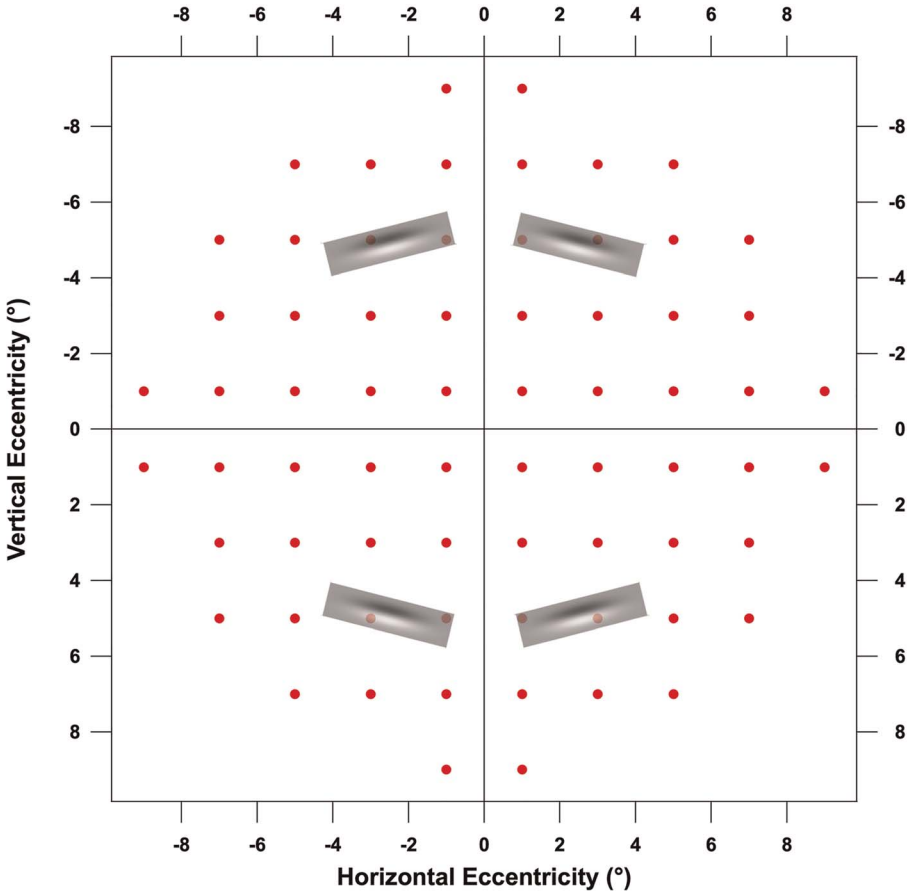

FIGURE 4. Four locations used for the elongated first derivative of Gaussian stimulus (rectangles), relative to the 10-2 locations (circles). The elongated sinusoidal stimulus was presented at only four locations to reduce the number of perimetric locations tested as compared with 10-2 grid. These four locations were selected with enough distance between two locations in the horizontal access, to avoid the overlap between the two stimuli. Horizontal and vertical eccentricities, in degrees, are represented in the *x*- and *y*-axes.

structural defects observed on the en face images of the nerve fiber bundles; an example is shown in Fig. 5. For the 37 control participants, the –0.4 log unit criterion was the only criterion that identified perimetric defects (in two control participants).

For the elongated sinusoidal stimulus, Fig. 6 shows results for the patients in the current study and the normative data for perimetric sensitivities from our prior study. Of 20 patients, 18 had at least one location with perimetric sensitivity that fell below the 2.5th percentile (Fig. 6). For 20 patients, the numbers with sensitivities below the 2.5th percentile were 14 (82%) at location 1, 11 (65%) at location 2, 8 (47%) at location 3, and 4 (24%) at location 4.

By using the gray scale (perimetric defect was defined based on the 2.5th percentile, as shown in Fig. 7), 15 of the new 20 patients with glaucoma were identified using total deviation, 17 using pattern deviation maps, and 13 patients using both total deviation and pattern deviation maps; an example is shown in Fig. 8. None of the control participants were identified with abnormal perimetric locations that were adjoining, when pattern deviation was applied. The 17 patients were also identified with perimetric defect in at least one location using the elongated sinusoidal stimulus.

When using the 2.5th percentile to define perimetric defect with blob stimulus and elongated sinusoidal stimulus, 17 and 18 patients were identified with perimetric defect, respectively. One of the three remaining patients had a very thin structural defect at the macula and was not identified by either the blob stimulus or the elongated sinusoidal stimulus. The other two patients had

TABLE 1. Patients identified by applying –0.4, –0.5, or –0.6 log unit criteria, for TD and PD maps

Criterion	Participants with perimetric defect identified using TD	Participants with perimetric defect identified using PD	Participants with perimetric defect identified using both TD and PD
–0.4 dB	23	23	23
–0.5 dB	22	20	19
–0.6 dB	20	16	16

PD = pattern deviation; TD = total deviation.

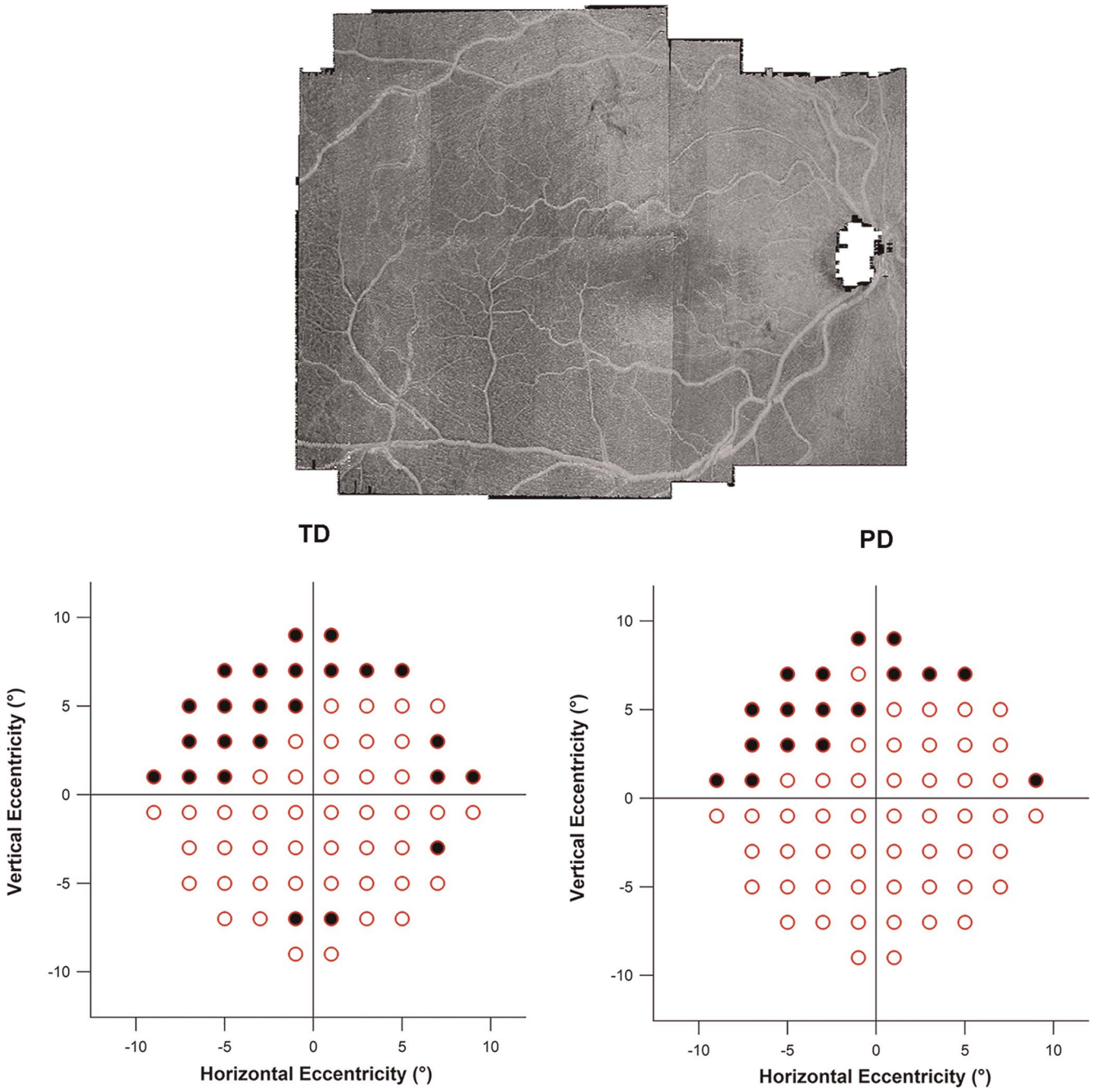

FIGURE 5. An example for one patient tested with the blob stimulus where structure-function agreement was good. The top panel shows an en face image of the retinal nerve fiber bundles, the left panel shows the total deviation map, and the right panel shows the pattern deviation map. Black circles indicate that the perimetric defect was deeper than –0.4 log units. Horizontal and vertical eccentricities are represented in *x*- and *y*-axes of the total deviation and pattern deviation plots. It can be observed that there was a good structure-function agreement in the area of glaucomatous defect.

a high height of hill of vision, but one of them was identified with the elongated sinusoidal stimulus.

When we averaged sensitivities for the four perimetric locations tested with blob stimuli, which were mostly covered by the elongated sinusoidal stimulus, we found similar results. Five patients with glaucoma were not identified as having sensitivity below the 5th percentile for controls. The average time to test the four locations with the elongated sinusoidal stimulus was approximately 1 minute and 10 seconds, whereas the average time for the testing 68 locations was approximately 5 minutes and 40 seconds.

DISCUSSION

Identifying glaucomatous damage to the macula has become important for the clinical diagnosis and management of patients

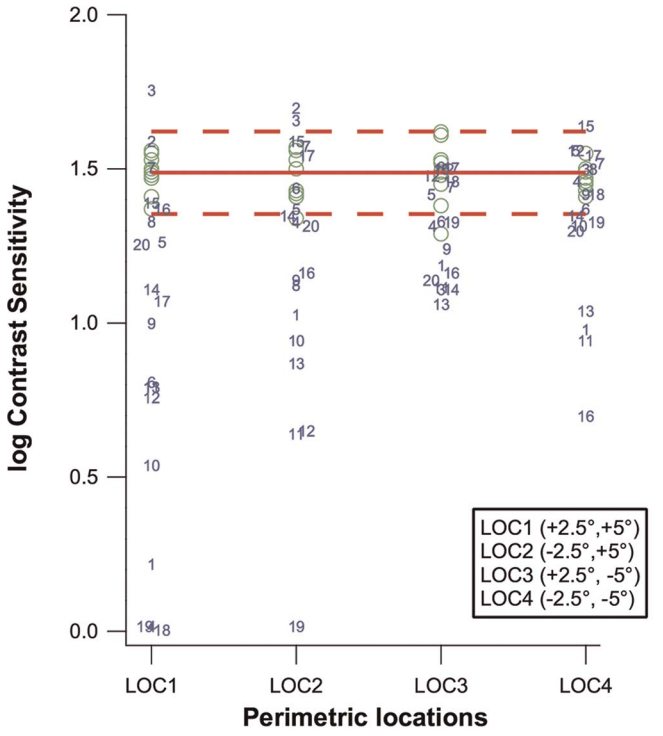

FIGURE 6. Contrast sensitivity data for the elongated first derivative Gaussian stimulus collected from control participants in our prior study[10] (circles) and from patients with glaucoma (numbers) in the current study. The *x*-axis indicates the eccentricities of the perimetric locations, and the *y*-axis indicates contrast sensitivity in log units. The dashed lines represent the 95% reference range, and the solid line represents mean sensitivity for the data of control participants. Perimetric defect was defined as at least one perimetric location that had perimetric sensitivity below the 2.5th percentile for the control participants.

with glaucoma. Recent studies demonstrated that there was a good structure-function agreement within the macula, using 10-2 grid.[1–5] However, it is a clinical challenge to assess patients with glaucoma by testing both 24-2 and 10-2 grids. A recent work suggested adding fixed perimetric locations to the center of the 24-2 grid (Sophia YU, et al. IOVS 2019;60:ARVO E-Abstract 2454), but there were no supporting structural data to assess the structure-function agreement. In the current study, the goal was to present a clinical approach with a good structure-function agreement within the macula in patients with glaucoma by decreasing the number of perimetric locations from 68 to 4.

The first step toward achieving the goal of this study was to refine a basis for customizing perimetric locations within the macula using blob stimuli, as previously presented.[10] After refining the basis with multiple criteria that defined the perimetric abnormality for a location, we found that the –0.4 criterion (0.4 log units lower than total deviation or pattern deviation values as in control participants) yielded better structure-function agreement than the other criteria (the –0.5 and –0.6 log units). By using the –0.4 criterion, 23 of 30 patients were identified with perimetric defect within the macula. However, all 30 patients had structural damage to the macula when we applied previously described criteria and methods[29] with asymmetry analysis of ganglion cell thickness using spectral-domain optical coherence tomography. Our laboratory has developed methods to reduce test-retest variability and improve structure-function agreement, which led to the use of a blob stimulus in this study. We built on a prior study[19] that had used blobs as a reference.

On the other hand, when the criterion of defining the abnormality for a blob stimulus at a given location was defined as any value lower than the 2.5th percentile (–0.25 log units), as derived from the control data for the small blob at that location, the correspondence between the structural and functional data was improved. By applying this criterion, there were 18 of the new 20 patients and 27 of the total 30 patients who were identified with perimetric defect within the macula. These perimetric defects corresponded to the structural defects. It is worthwhile to mention that, in the prior study, we compared the effect of ganglion cell body displacement on our approach and found that it made no difference between using the model with and without ganglion cell body displacement.[10] The success of the elongated sinusoidal stimulus confirms this finding.

This refinement was used as a reference for comparison to the performance of the four locations with the elongated sinusoidal

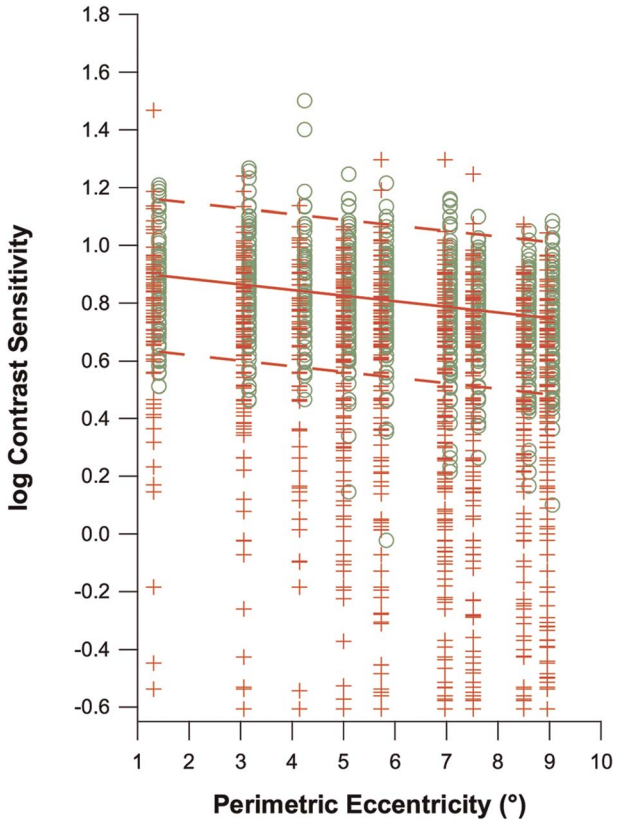

FIGURE 7. The 95% reference range (dashed lines) and mean sensitivity at each eccentricity (solid line) from control participants for the blob stimulus at the 10-2 locations. The *x*-axis represents perimetric eccentricity in degrees, and the *y*-axis represents perimetric sensitivity in log Weber contrast. Crosses represent data derived from patients at different eccentricities. Circles indicate perimetric sensitivities derived from control participants. Linear regression of sensitivity versus eccentricity was used to define mean normal, and ±1.96 times the standard deviation of residuals was used to define the 95% reference range. The 2.5th percentile was used to define perimetric abnormality, based on which the gray-scale plots for control participants and patients with glaucoma were created. It can be observed that 3% of data points (from seven control participants) fell below the 2.5th percentile; these points were not for adjoining locations. Data points for patients were slightly shifted to the left on the *x*-axis to improve the clarity of the data presentation.

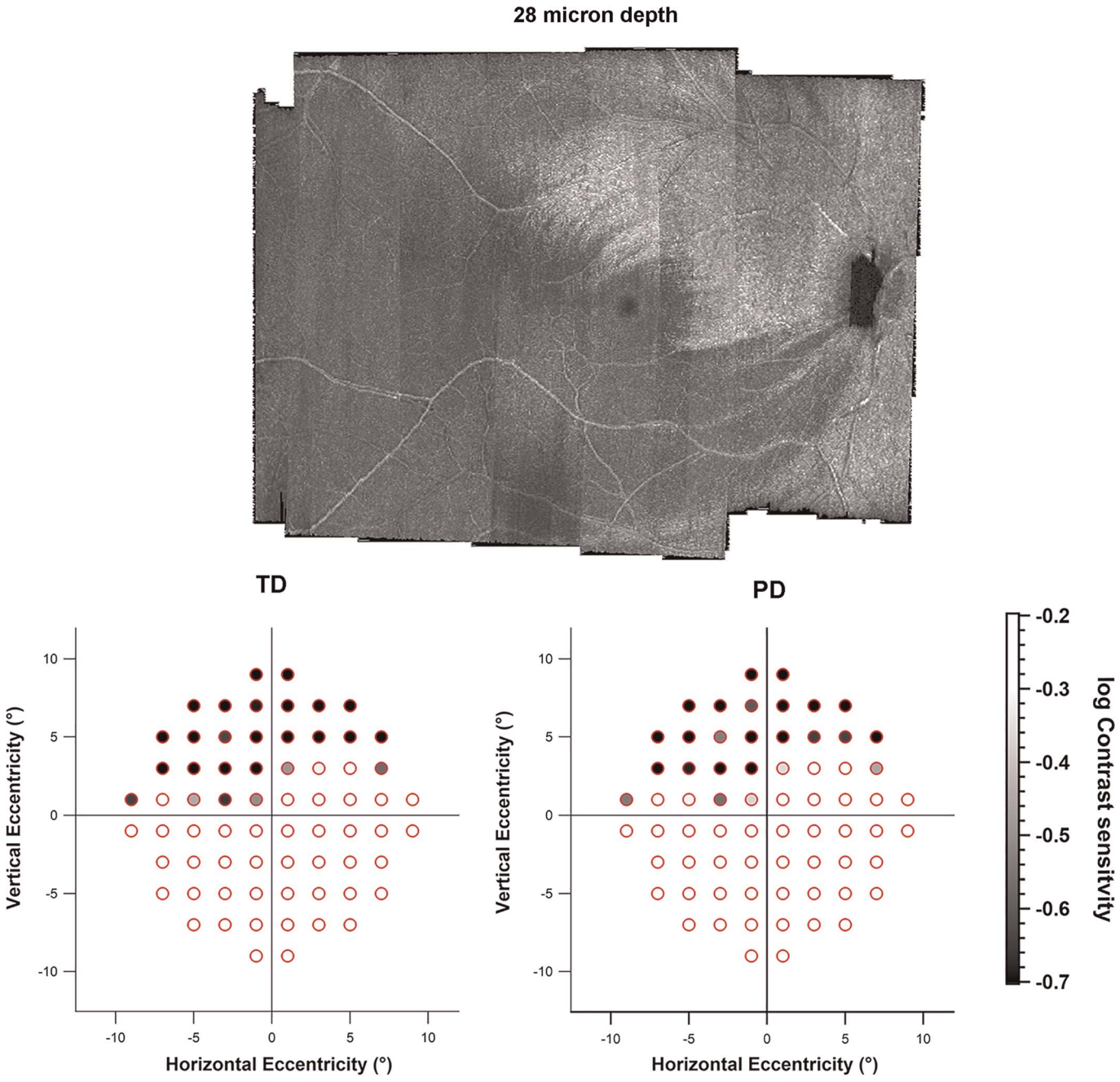

FIGURE 8. An example for one patient tested with the small blob stimulus where structure-function agreement was good. Top is an en face image of the retinal nerve fiber bundles, middle is the total deviation map, and right is the pattern deviation map. Gray scale on the right represents the range of total deviation and pattern deviation values that we restricted to start from –0.25 (white, less perimetric defect) to –0.7 log units (black, deeper perimetric defect). Vertical and horizontal eccentricities are represented in *x*-and *y*-axes of the total deviation and pattern deviation plots.

stimulus. The approach of using the 2.5th percentile was applied for the control participants to define perimetric defects. There were 18 of 20 patients who were identified with perimetric defects (Fig. 6) with the elongated sinusoidal stimulus. The good agreement between perimetric and structural defects was similar for both blob and elongated sinusoidal stimuli, but the latter was presented at only four locations, whereas the small blob was presented at 68 locations within the macula. This indicates that we were successful in choosing locations for the elongated sinusoidal stimulus that identified perimetric defects within the macula.

This study extends the result of previously published work that demonstrated that the elongated sinusoidal stimulus yielded reduced perimetric sensitivities when presented at customized locations based on areas of glaucomatous damage, including stimuli presented at the macula.[10] Although the elongated sinusoidal stimulus is much larger than the size III Goldmann stimulus, large sinusoidal stimuli have been shown to yield similar defects in patients with glaucoma.[12–15] We concluded that the use of en face images could identify functional defects that fell between the 24-2 locations by using targeted perimetry. For this reason, we

expect high sensitivity of en face images for detecting functional defect. However, assessment of the generalizability of this finding would require a much larger data set than the sample size in the current study.

Similarly, for specificity of the novel stimuli, a much larger sample would be needed. We found that, for the blob stimuli, none of the 37 controls were failed by the –0.5 log unit criterion. This implies a 95% confidence interval on specificity of 88 to 100%; if none of a sample size of 92 was failed then that would shrink the confidence interval to the range of 95 to 100%, and 0 of 475 would be needed for the range of 99 to 100%.

Our elongated sinusoidal stimulus was shown to have low sensitivities at locations of glaucomatous damage to retinal nerve fiber layer.[25] The spatial frequency was chosen to avoid a large size while reducing the effects of blur from peripheral defocus or astigmatism.[19] The flicker rate was chosen so that the data should adhere to Weber's law[21] and to provide the advantages of a large area of cortical pooling.[15]

Other studies suggested the use of customized perimetric location to predict the functional loss by using the measurements of retinal nerve fiber layer thickness with optical coherence tomography.[30,31] These studies, however, did not provide spatial comparison between functional and structural measurements. The original approach of the current study was that the structural information derived from the en face images of the retinal nerve fiber bundles could guide perimetry to customize perimetric locations to identify functional defects, leading to spatial structure-function comparison. However, we found that the locations tested with the elongated sinusoidal stimulus could potentially be implemented at fixed locations (without the use of customized locations) within the macula to identify glaucomatous damage and led to a good structure-function agreement in our sample. This can potentially increase the confidence in decision making for clinicians when diagnosing and managing patients with glaucoma.

There were two limitations to this study. First, the sample size was relatively small; therefore, more studies are warranted with larger sample sizes to confirm our results or explore more aspects of our approach. Second, we used our laboratory apparatus with specific features of the visual field testing. However, the testing protocol used in this study could be used as a framework for other studies that apply similar testing protocols with clinical settings.

In conclusion, the use of the 2.5th percentile to define perimetric defects demonstrated a good structure-function agreement within the macula for both blob and elongated sinusoidal stimuli. The elongated sinusoidal stimulus, however, was presented at only four perimetric locations as compared with 68 locations for the small blob stimulus. This is a tremendous reduction in the number of perimetric locations while maintaining a good structure-function agreement. This demonstrates a potential for this new stimulus in the next generation of the clinical perimetry. Further investigation is warranted to examine the performance of the elongated sinusoidal stimulus at the four locations suggested in this study.

ARTICLE INFORMATION

Submitted: June 12, 2020

Accepted: December 23, 2020

Funding/Support: National Eye Institute (National Institutes of Health grant EY024542; to WHS).

Conflict of Interest Disclosure: None of the authors have reported a financial conflict of interest.

Author Contributions: Conceptualization: MSA, WHS, BJK; Data Curation: MSA, WHS, BJK; Formal Analysis: MSA, WHS; Funding Acquisition: WHS; Investigation: MSA, WHS; Methodology: MSA, WHS, BJK; Resources: BJK; Supervision: WHS, BJK; Visualization: MSA, BJK; Writing – Original Draft: MSA; Writing – Review & Editing: WHS, BJK.

REFERENCES

1. Kanadani FN, Hood DC, Grippo TM, et al. Structural and Functional Assessment of the Macular Region in Patients with Glaucoma. Br J Ophthalmol 2006;90:1393–7.

2. Raza AS, Cho J, de Moraes CG, et al. Retinal Ganglion Cell Layer Thickness and Local Visual Field Sensitivity in Glaucoma. Arch Ophthalmol 2011;129:1529–36.

3. Hori N, Komori S, Yamada H, et al. Assessment of Macular Function of Glaucomatous Eyes by Multifocal Electroretinograms. Doc Ophthalmol 2012;125:235–47.

4. Takahashi M, Omodaka K, Maruyama K, et al. Simulated Visual Fields Produced from Macular RNFLT Data in Patients with Glaucoma. Curr Eye Res 2013;38:1133–41.

5. Lee JW, Morales E, Sharifipour F, et al. The Relationship between Central Visual Field Sensitivity and Macular Ganglion Cell/Inner Plexiform Layer Thickness in Glaucoma. Br J Ophthalmol 2017;101:1052–8.

6. Wu Z, Medeiros FA, Weinreb RN, et al. Performance of the 10-2 and 24-2 Visual Field Tests for Detecting Central Visual Field Abnormalities in Glaucoma. Am J Ophthalmol 2018;196:10–7.

7. Hood DC, Thenappan AA, Tsamis E, et al. An Evaluation of a New 24-2 Metric for Detecting Early Central Glaucomatous Damage. Am J Ophthalmol 2020;223:119–28.

8. Ashimatey BS, Swanson WH. Between-subject Variability in Healthy Eyes as a Primary Source of Structural-functional Discordance in Patients with Glaucoma. Invest Ophthalmol Vis Sci 2016;57:502–7.

9. Phu J, Kalloniatis M. Ability of 24-2c and 24-2 Grids to Identify Central Visual Field Defects and Structure-function Concordance in Glaucoma and Suspects. Am J Ophthalmol 2020;219:317–31.

10. Alluwimi MS, Swanson WH, Malinovsky VE, et al. A Basis for Customising Perimetric Locations within the Macula in Glaucoma. Ophthalmic Physiol Opt 2018;38:164–73.

11. Iikawa R, Togano T, Sakaue Y, et al. Estimation of the Central 10-degree Visual Field Using En-face Images Obtained by Optical Coherence Tomography. PLoS One 2020;15:e0229867.

12. Artes PH, Hutchison DM, Nicolela MT, et al. Threshold and Variability Properties of Matrix Frequency-doubling Technology and Standard Automated Perimetry in Glaucoma. Invest Ophthalmol Vis Sci 2005;46:2451–7.

13. Sun H, Dul MW, Swanson WH. Linearity Can Account for the Similarity among Conventional, Frequency-doubling, and Gabor-based Perimetric Tests in the Glaucomatous Macula. Optom Vis Sci 2006;83:455–65.

14. Swanson WH, Malinovsky VE, Dul MW, et al. Contrast Sensitivity Perimetry and Clinical Measures of Glaucomatous Damage. Optom Vis Sci 2014;91:1302–11.

15. Swanson WH, King BJ. Comparison of Defect Depths for Sinusoidal and Circular Perimetric Stimuli in Patients with Glaucoma. Ophthalmic Physiol Opt 2019;39:26–36.

16. Girard MJ, Strouthidis NG, Ethier CR, et al. Shadow Removal and Contrast Enhancement in Optical Coherence Tomography Images of the Human Optic Nerve Head. Invest Ophthalmol Vis Sci 2011;52:7738–48.

17. Vermeer KA, Mo J, Weda JJ, et al. Depth-resolved Model-based Reconstruction of Attenuation Coefficients in Optical Coherence Tomography. Biomed Opt Express 2013;5:322–37.

18. Ashimatey BS, King BJ, Malinovsky VE, et al. Novel Technique for Quantifying Retinal Nerve Fiber Bundle Abnormality in the Temporal Raphe. Optom Vis Sci 2018;95:309–17.

19. Horner DG, Dul MW, Swanson WH, et al. Blur-resistant Perimetric Stimuli. Optom Vis Sci 2013;90:466–74.

20. Ashimatey BS, King BJ, Burns SA, et al. Evaluating Glaucomatous Abnormality in Peripapillary Optical Coherence Tomography Enface Visualisation of the Retinal Nerve Fibre Layer Reflectance. Ophthalmic Physiol Opt 2018;38:376–88.

21. Swanson WH, Dul MW, Horner DG, et al. Assessing Spatial and Temporal Properties of Perimetric Stimuli for Resistance to Clinical Variations in Retinal Illumination. Invest Ophthalmol Vis Sci 2014;55:353–9.

22. Gardiner SK, Swanson WH, Goren D, et al. Assessment of the Reliability of Standard Automated Perimetry in Regions of Glaucomatous Damage. Ophthalmology 2014;121:1359–69.

23. Swanson WH, Horner DG, Dul MW, et al. Choice of Stimulus Range and Size Can Reduce Test-retest Variability in Glaucomatous Visual Field Defects. Transl Vis Sci Technol 2014;3:6.

24. Swanson WH, Sun H, Lee BB, et al. Responses of Primate Retinal Ganglion Cells to Perimetric Stimuli. Invest Ophthalmol Vis Sci 2011;52:764–71.

25. Alluwimi MS, Swanson WH, Malinovsky VE, et al. Customizing Perimetric Locations Based on En Face Images of Retinal Nerve Fiber Bundles with Glaucomatous Damage. Transl Vis Sci Technol 2018;7:5.

26. Zeppieri M, Brusini P, Parisi L, et al. Pulsar Perimetry in the Diagnosis of Early Glaucoma. Am J Ophthalmol 2010;149:102–12.

27. Hu R, Wang C, Racette L. Comparison of Matrix Frequency-doubling Technology Perimetry and Standard Automated Perimetry in Monitoring the Development of Visual Field Defects for Glaucoma Suspect Eyes. PLoS One 2017;12:e0178079.

28. Hood DC, Nguyen M, Ehrlich AC, et al. A Test of a Model of Glaucomatous Damage of the Macula with High-density Perimetry: Implications for the Locations of Visual Field Test Points. Transl Vis Sci Technol 2014;3:5.

29. Alluwimi MS, Swanson WH, King BJ. Identifying Glaucomatous Damage to the Macula. Optom Vis Sci 2018;95:96–105.

30. Zhu H, Crabb DP, Schlottmann PG, et al. Predicting Visual Function from the Measurements of Retinal Nerve Fiber Layer Structure. Invest Ophthalmol Vis Sci 2010;51:5657–66.

31. Ballae Ganeshrao S, Turpin A, McKendrick AM. Sampling the Visual Field Based on Individual Retinal Nerve Fiber Layer Thickness Profile. Invest Ophthalmol Vis Sci 2018;59:1066–74.